Cell Metabolism
Article

Loss of TGH/Ces3 in Mice Decreases Blood Lipids, Improves Glucose Tolerance, and Increases Energy Expenditure

Enhui Wei,[1,3] Yassine Ben Ali,[1,3] James Lyon,[4] Huajin Wang,[2,3] Randy Nelson,[3] Vernon W. Dolinsky,[1] Jason R.B. Dyck,[1] Grant Mitchell,[5] Gregory S. Korbutt,[4] and Richard Lehner[1,2,3,*]
[1]Department of Pediatrics
[2]Department of Cell Biology
[3]Group on Molecular and Cell Biology of Lipids
University of Alberta, Edmonton, AB T6G 2S2, Canada
[4]Department of Surgery, University of Alberta, Edmonton, AB T6G 2E1, Canada
[5]Department of Pediatrics, CHU Sainte-Justine, Université de Montreal, Montreal, QC H3T 1C5, Canada
*Correspondence: richard.lehner@ualberta.ca
DOI 10.1016/j.cmet.2010.02.005

SUMMARY

Excessive accumulation of triacylglycerol in peripheral tissues is tightly associated with obesity and has been identified as an independent risk factor for insulin resistance, type 2 diabetes, and cardiovascular complications. Here we show that ablation of carboxylesterase 3 (Ces3)/triacylglycerol hydrolase (TGH) expression in mice ($Tgh^{-/-}$) results in decreased plasma triacylglycerol, apolipoprotein B, and fatty acid levels in both fasted and fed states. Despite the attenuation of very low-density lipoprotein secretion, TGH deficiency does not increase hepatic triacylglycerol levels. $Tgh^{-/-}$ mice exhibit increased food intake, respiratory quotient, and energy expenditure without change in body weight. These metabolic changes are accompanied by improved insulin sensitivity and glucose tolerance. $Tgh^{-/-}$ mice have smaller sized pancreatic islets but maintain normal glucose-stimulated insulin secretion. These studies demonstrate the potential of TGH as a therapeutic target for lowering blood lipid levels.

INTRODUCTION

The major function of hepatic very low-density lipoproteins (VLDLs) is to deliver triacylglycerol (TG) from the liver to peripheral tissues. Increased plasma TG levels represent an independent risk factor for cardiovascular disease (Carmena et al., 2004; Havel, 1990). Additionally, insulin resistance, hypertension, and visceral obesity are also characterized by elevated plasma concentration of TG-rich lipoproteins (Carmena et al., 2004; Ginsberg et al., 2005; Schaefer et al., 2002). Because of the potential for pharmacological intervention, the mechanism of VLDL assembly and secretion in the liver has attracted considerable interest (Chahil and Ginsberg, 2006; Cuchel et al., 2007; Lieu et al., 2003).

Accumulating evidence suggests that the formation of apolipoprotein B (apoB)-containing lipoproteins is accomplished through two steps (Fisher and Ginsberg, 2002; Kulinski et al., 2002; Raabe et al., 1999; Vukmirica et al., 2003). Initially, a primordial relatively lipid-poor particle is formed during apoB translocation into the lumen of the endoplasmic reticulum (ER), and this process requires active new synthesis of lipids, including TG. Subsequently, apoB acquires the bulk of core lipids (mainly TG) to form a mature VLDL. The central role of TG in the assembly and secretion of apoB lipoproteins has been demonstrated in cultured hepatocytes (Fisher and Ginsberg, 2002; Gibbons et al., 2004). The majority (60%–70%) of VLDL-TG secreted from hepatocytes is derived from stored TG via a process of lipolysis and re-esterification (Gibbons et al., 2000, 2004; Wiggins and Gibbons, 1992; Yang et al., 1995, 1996).

An ER-localized triacylglycerol hydrolase (TGH), also termed carboxylesterase 3 (Ces3) in mice and carboxylesterase 1 (CES1) in humans, has been suggested to play a role in the provision of substrates for the assembly of apoB-containing lipoproteins (Dolinsky et al., 2004a, 2004b; Lehner and Verger, 1997). Expression of TGH cDNA in McArdle RH7777 cells increased lipolysis of preformed TG stores and augmented TG secretion and levels of apoB100 in the VLDL density range (Gilham et al., 2005; Lehner and Vance, 1999). Fasting plasma TG and apoB levels were increased in transgenic mice that express human TGH specifically in the liver (Wei et al., 2007a). Inhibition of lipolysis in intact primary rat hepatocytes by a cell-permeable TGH-specific inhibitor resulted in decreased secretion of apoB and TG (Gilham et al., 2003). These data support an active role for TGH in the mobilization of intracellular TG for VLDL assembly.

ApoB lipidation is a potential pharmacological target for the treatment of hypertriglyceridemia and associated cardiovascular and metabolic diseases. One major concern is that inhibition of hepatic VLDL secretion may lead to hepatic steatosis. Such condition has been observed upon chemical inhibition or genetic disruption of microsomal triglyceride transfer protein (MTP) (Chandler et al., 2003; Cuchel et al., 2007; Raabe et al., 1999). Hepatic steatosis is strongly associated with decreased insulin sensitivity (Marchesini et al., 2005; Petersen and Shulman, 2006; Savage et al., 2007), although recent data suggest that

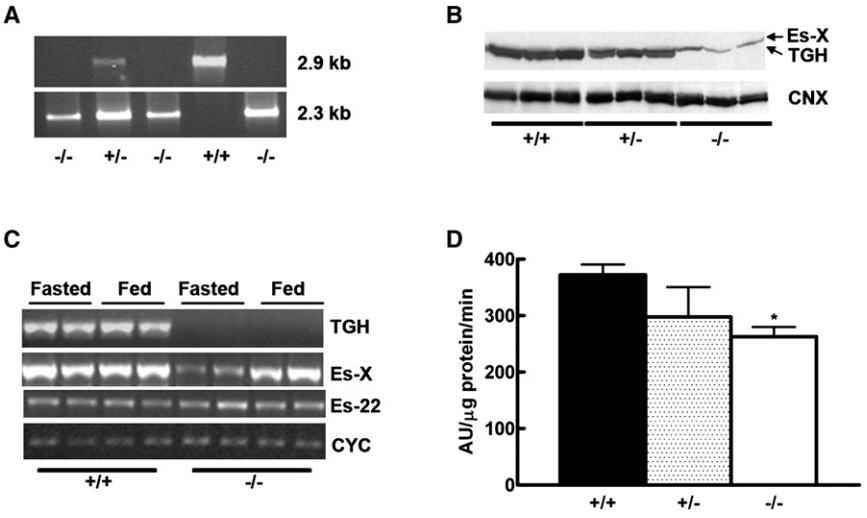

Figure 1. Generation of TGH-Deficient Mice

(A) PCR of genomic DNA.

(B and C) Absence of TGH protein (B) and mRNA (C) in homozygous TGH null mice. Es-x is a related carboxylesterase migrating at higher M_r due to additional glycosylation and is recognized by the polyclonal anti-TGH peptide antibodies.

(D) Carboxylesterase activities in total liver homogenates. Bars in (D) represent means ± SD. *p < 0.05 versus WT.

accumulation of hepatic TG stores alone may not be sufficient to cause insulin resistance (Monetti et al., 2007).

To test the hypothesis that attenuation of TGH expression leads to decreased VLDL secretion in vivo, we generated TGH knockout mice. We examined the phenotype of these mice with respect to VLDL secretion, hepatic lipid accumulation, insulin regulation of glucose homeostasis, and the effect on whole-body energy utilization.

RESULTS

Decreased Liver Lipase Activity in *Tgh*$^{-/-}$ Mice

The strategy that we used to generate TGH null mice is shown in Figure S1 (available online). Disruption of TGH in mice was demonstrated by PCR of mouse genomic DNA (Figure 1A). To verify the absence of the TGH protein, liver homogenates were analyzed by immunoblotting with an antiserum that was raised against the C-terminal 14 amino acid residues of mouse TGH (Wang et al., 2007). TGH protein was undetectable in *Tgh*$^{-/-}$ mice, and normal levels were maintained in *Tgh*$^{+/-}$ mice (Figure 1B). The peptide used for immunization of rabbits shares 10 out of 14 residues with a related family member carboxylesterase 1 (Es-x), which is detected as the higher-migrating immunoreactive band (Figure 1B). Figure 1C shows that specific targeting was achieved since the expression of *Es-x* and another carboxylesterase *Es-22* was not affected. These two genes are located in the same carboxylesterase gene cluster as TGH and share 75% identity with TGH including 100% in the targeted exon 5 (Dolinsky et al., 2004b). Ablation of *Tgh* expression resulted in 30% reduction of the carboxylesterase activity in liver homogenates (Figure 1D).

Decreased Plasma Lipid and ApoB in *Tgh*$^{-/-}$ Mice

Next we tested the hypothesis that TGH is involved in the provision of substrates for VLDL secretion in vivo. Plasma phospholipid (PL) concentration was not significantly altered in *Tgh*$^{-/-}$ mice compared with WT controls (Table 1). TGH deficiency led to decreased fasting plasma concentrations of unesterified (free) cholesterol (FC), cholesteryl esters (CE), and TG by 17%, 25%, and 50%, respectively, and by 27%, 33%, and 25% in the fed state (Table 1). Decreased plasma lipid levels were mainly due to reduction of VLDL-sized particles (Figures 2A and 2B). Correspondingly, plasma apoB100 levels were markedly decreased in *Tgh*$^{-/-}$ mice in both fasted (Figure 2C) and fed (Figure 2D) states. Plasma apoB48 levels were not significantly changed, possibly due to the ability of this protein to be secreted on TG-poor particles.

To evaluate whether the decreased plasma apoB100 and TG concentrations are a result of reduced secretion or increased catabolism, we analyzed apoB and TG secretion in vivo. [^{35}S]Methionine was injected into the tail vein of mice, followed by detergent P-407 administration to block lipolysis of secreted lipoproteins by plasma lipases, therefore attenuating the uptake of secreted lipoproteins through the LDL receptor pathway. Secretion of newly synthesized labeled apoB and TG was in a linear range for at least 3 hours following administration of the radiolabeled amino acid (data not shown). The secretion of newly synthesized apoB100 was significantly decreased in *Tgh*$^{-/-}$ mice (Figure 2E). Analysis of densities of newly secreted apoB lipoproteins revealed that all apoB100 is present in lipid enriched fractions, but the levels of apoB100 in all fractions were lower in *Tgh*$^{-/-}$ mice (Figure 2F), indicating compromised apoB100 lipidation. Secretion of newly synthesized apoB48 was not affected in *Tgh*$^{-/-}$ mice (Figure 2E), and apoB48-containing particles were secreted from *Tgh*$^{-/-}$ mice with a wider density range compared to WT mice (Figure 2F). Despite decreased lipidation and secretion of apoB100 from *Tgh*$^{-/-}$ mice, TG secretion rates from WT and *Tgh*$^{-/-}$ mice were similar (214 ± 15.5 and 220 ± 65 mg/dl/hr, respectively) suggesting compensatory TG association with apoB48-containing lipoproteins. MTP is responsible for the transfer of lipids to nascent apoB and therefore is believed to represent the rate-limiting step in VLDL assembly and secretion (Hussain et al., 2003; Kulinski et al., 2002; Raabe et al., 1999; Tietge et al., 1999; Wang et al., 1996). The level of MTP was not altered in *Tgh*$^{-/-}$ mice, suggesting that the observed decrease in VLDL secretion is independent of MTP function (Figure S2).

Decreased VLDL Secretion from Isolated Hepatocytes

To further assess the mechanism of TGH-mediated mobilization of stored cellular TG for VLDL assembly, primary mouse hepatocytes were isolated and lipid turnover studies were performed. Hepatocytes were incubated in media containing [^{3}H]oleic acid (OA) and [^{14}C]glycerol. *Tgh*$^{-/-}$ hepatocytes exhibited 28.8% and 41.1% decrease of [^{3}H]OA-derived TG secretion during

Table 1. Phenotypic Comparison of Wild-Type and *Tgh*$^{-/-}$ Mice

	Fasted		Fed	
	WT	*Tgh*$^{-/-}$	WT	*Tgh*$^{-/-}$
Plasma TG (mg/dl)	32.08 ± 21.17	22.79 ± 13.39*	38.69 ± 8.34	29.09 ± 2.87*
Plasma FC (mg/dl)	42.99 ± 8.80	37.73 ± 12.00*	41.20 ± 2.68	29.89 ± 4.32*
Plasma CE (mg/dl)	52.61 ± 12.22	42.80 ± 12.82**	46.48 ± 5.05	31.00 ± 7.20*
Plasma PL (mg/dl)	84.24 ± 29.66	89.20 ± 38.19	75.62 ± 9.77	63.94 ± 6.43
Liver TG (μg/mg protein)	257.94 ± 180.23	203.14 ± 108.30	23.52 ± 18.89	7.03 ± 4.27*
Liver FC (μg/mg protein)	16.99 ± 1.1	16.64 ± 1.17	15.20 ± 2.16	14.58 ± 2.32
Liver CE (μg/mg protein)	7.31 ± 3.89	4.49 ± 1.17	1.20 ± 0.51	0.92 ± 0.23
Liver PL (μg/mg protein)	76.46 ± 14.03	82.42 ± 11.79	60.48 ± 13.62	56.58 ± 21.89
Blood glucose (mmol/L)	2.57 ± 0.59	2.63 ± 0.45	6.60 ± 0.95	5.25 ± 0.59
Adiponectin (μg/ml)	7.20 ± 4.40	5.40 ± 1.79	8.80 ± 2.45	5.35 ± 1.73*
Leptin (ng/ml)	3.00 ± 2.44	3.33 ± 2.15	2.67 ± 1.57	2.91 ± 0.87
Insulin (pg/ml)	770.3 ± 387.1	396.3 ± 291.5	375.8 ± 222.4	419.2 ± 194.1
Resistin (pg/ml)	626.3 ± 330.4	441.3 ± 151.0	494.7 ± 206.2	691.0 ± 231.6

Male wild-type and *Tgh*$^{-/-}$ mice (14- to 16-week old, n = 8–12 of each group) were fed a standard chow diet and were terminated in the fasted (fasting for 16 hr) or fed (normal access to chow diet) state. Each value represents the mean ± SD. *$p < 0.05$, **$p < 0.01$ versus WT.

pulse or chase periods, respectively (Figure 3A). The secretion of [^{14}C]glycerol-derived TG from *Tgh*$^{-/-}$ hepatocytes was also significantly reduced (Figure 3B). Phosphatidylcholine (PC) (Figures 3C and 3D) and CE (Figure 3E) secretion was not altered by the ablation of *Tgh* expression.

The consequence of ablation of *Tgh* expression on cellular and secreted lipid mass in isolated hepatocytes was evaluated following incubation with 0.4 mM OA for 16 hr. OA supplementation increased TG mass in hepatocytes isolated from *Tgh*$^{-/-}$ mice compared to hepatocytes isolated from WT mice in agreement with the role of the enzyme in TG turnover (Figure 3F). Additionally, intracellular CE levels increased from 2.08 ± 0.50 to 4.15 ± 0.55 μg/mg protein ($p < 0.01$) in TGH-deficient hepatocytes upon OA supplementation. Cellular FC and PL mass were not affected by the ablation of *Tgh* expression (data not shown). In agreement with pulse-chase studies, primary hepatocytes from TGH-deficient mice secreted less TG into the media (Figure 3G), which could be mainly attributed to decreased VLDL-TG secretion (Figure 3H). In the absence of TGH, the secretion of apoB100 from isolated hepatocytes was substantially reduced, while the secretion of apoB48 was reduced only to a lesser degree (Figure 3I). Secreted albumin levels were not affected by TGH deficiency, indicating that the general secretory machinery in primary hepatocytes remained unchanged.

Decreased VLDL Secretion from Human Hepatocytes

In order to examine whether decreased VLDL secretion due to ablation of TGH activity in mice would be recapitulated in humans, we have utilized primary human hepatocytes to study the effect of attenuation of TGH activity on VLDL and apoB secretion. Treatment of primary human hepatocytes with a specific TGH inhibitor GR148672X (Gilham et al., 2003; Wei et al., 2007b) reduced secretion of [^{3}H]OA-labeled TG and [^{14}C]glycerol-labeled TG in both pulse and chase periods (Figures 3J and 3K) but did not alter the secretion of labeled PC (data not shown). In agreement with radiolabeling studies, TGH inhibitor reduced secretion of TG mass both in the presence and absence of exogenously supplied OA by 40% and 50%, respectively (Figure 3L). ApoB100 secretion was concomitantly decreased by 25% ($p < 0.05$) (Figure 3M). Lipid mass analysis showed that TGH inhibitor did not alter the cell TG level with OA loading for 4 hr; however, the TG turnover was significant decreased in the presence of TGH inhibitor (Figure 3N). These results provide strong evidence for the role of TGH in VLDL secretion in humans.

Absence of Fatty Liver in *Tgh*$^{-/-}$ Mice

One possible side effect of decreasing hepatic lipolysis and VLDL secretion is hepatic steatosis. The percentage of liver weight with respect to body weight in TGH-deficient mice was reduced by 11.4% (4.02 ± 0.19 [WT] versus 3.56 ± 0.19 [KO], $p < 0.05$) and 19.6% (4.96 ± 0.32 [WT] versus 3.99 ± 0.31 [KO], $p < 0.01$) in the fasted and fed states, respectively. Livers from *Tgh*$^{-/-}$ mice that were fasted for 16 hr had lipid storage comparable to that of WT mice but exhibited significantly decreased TG mass in mice that had normal access to chow diet (Table 1). Similar results were obtained in females (data not shown). One reason for lack of hepatic TG accumulation in *Tgh*$^{-/-}$ mice in vivo despite attenuated VLDL secretion could be through decreased lipogenesis. Fatty acid synthase (FAS), stearoyl-coenzyme A desaturase 1 (SCD-1), and acylCoA:diacylglycerol acyltransferase (DGAT) catalyze committed steps in lipogenesis (Chen and Farese, 2005; Millar et al., 2006; Owen and Zammit, 1997; Smith et al., 2000; Stone et al., 2004). TGH deficiency did not affect TG synthesis from exogenously supplied fatty acid in isolated primary hepatocytes (Figure S3A) or the hepatic expression of *Fas* or *Dgat*, while *Scd-1* expression was decreased in fasted TGH KO mice (Figure S3B). Expression levels of other genes encoding lipolytic enzymes including arylacetamide deacetylase (AADA), adipose triglyceride lipase (ATGL), and hormone-sensitive lipase (HSL) were not altered in the livers of fasted TGH null mice (Figure S3B). The expression of *Aada* and *Atgl* was increased in the fed state of *Tgh*$^{-/-}$ mice

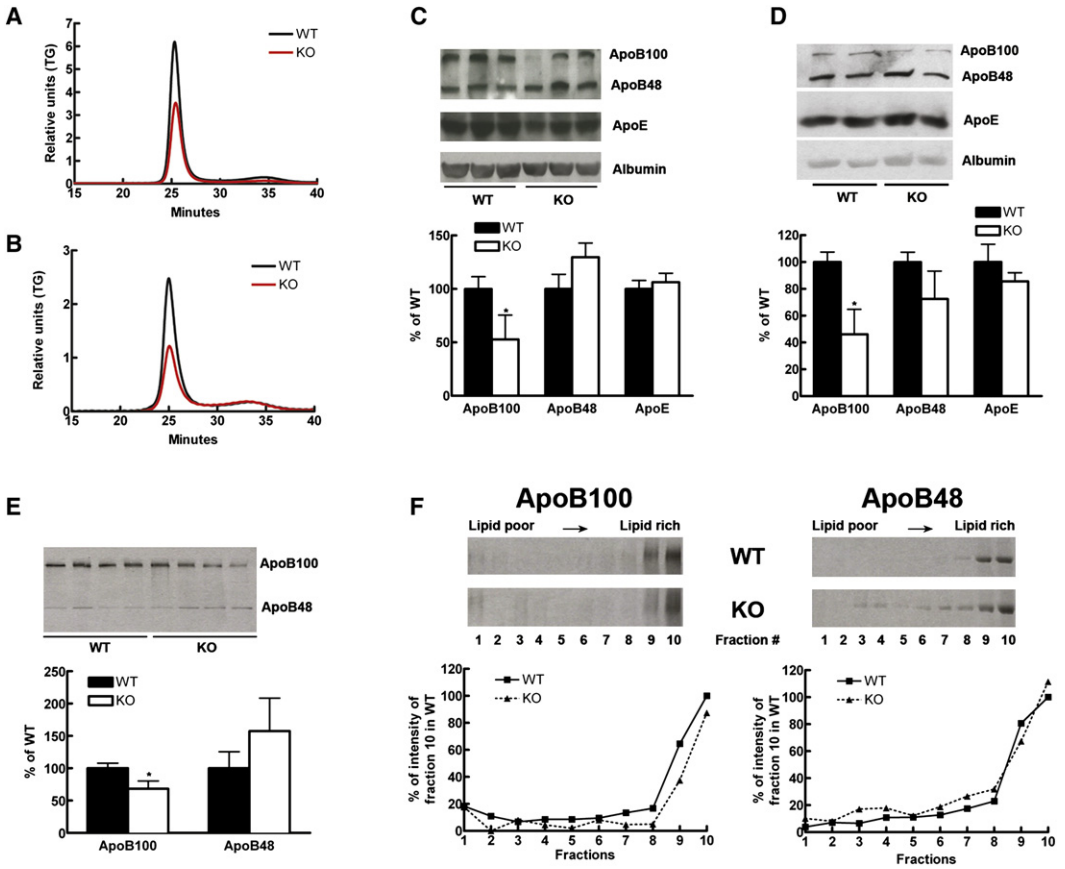

Figure 2. Decreased Plasma Triacylglycerol, ApoB100 Levels, and Reduced In Vivo ApoB100 Secretion in TGH-Deficient Mice

(A–D) Plasma was collected from 12- to 14-week-old male mice, n = 6 for each genotype. Pooled plasma from fasted (A) and fed (B) mice was subjected to analyses of TG content in lipoprotein fractions by fast-protein liquid chromatography. Two microliters of plasma from fasted (C) and fed (D) 12- to 14-week-old male mice were electrophoresed in SDS 4%–15% gradient polyacrylamide gels; proteins were transferred to nitrocellulose membranes; and apoB, apoE, and albumin levels were determined by immunoblotting.

(E) Decreased apoB100 secretion in vivo in *Tgh*$^{-/-}$ mice. Male mice were fasted for 4 hr, after which 200 μl of PBS containing 250 μCi of [^{35}S]methionine was injected into a tail vein and P-407 (1 g/kg body weight) in saline was injected intraperitoneally. The animals were euthanized after 2 hr, apoB was immunoprecipitated from 100 μl of plasma and electrophoresed on SDS 5% polyacrylamide gels, and the gels were dried and exposed to X-ray films.

(F) Decreased lipidation of apoB in *Tgh*$^{-/-}$ mice. Density of secreted newly synthesized apoB from pooled plasma from mice described above (E) was analyzed by ultracentrifugation. Relative intensities of the immunoreactive or radioactive bands were determined by densitometry using Bio-Rad Quantity One software. The ratio of specific apolipoprotein to albumin intensity in WT mice was assigned as 100%. Bars in (C)–(E) represent means ± SD. *$p < 0.05$, **$p < 0.01$ versus WT.

(Figure S3B), which could be one of the reasons for the observed lower hepatic TG levels (Table 1).

The liver can also be protected from excessive TG accumulation through diverting fatty acids into oxidation. Attenuation of *Tgh* expression resulted in increased β-oxidation in primary hepatocytes (Figure S3C), which was paralleled by augmented mRNA levels of hepatic enzymes involved in the mitochondrial β-oxidation of fatty acids, carnitine palmitoyltransferase I (CPT-I), and long-chain acyl-CoA dehydrogenase (LCAD) in fasted TGH null mice (Figures S3D and S3E). Messenger RNA levels of acyl-CoA oxidase (ACO), an enzyme that participates in the peroxisomal fatty acid oxidation, was not affected by the disruption of the *Tgh* gene in either the fasted or the fed state (Figure S3F). These results indicate that attenuation of *Tgh* expression results in increased channeling of fatty acids into oxidation.

Decreased Plasma Fatty Acid Levels in *Tgh*$^{-/-}$ Mice

TGH is also expressed in white adipose tissue (WAT), where it may participate in TG turnover and fatty acid efflux (Dolinsky et al., 2001; Soni et al., 2004; Wei et al., 2007b). Therefore, another possible explanation for the absence of hepatic neutral lipid accumulation in *Tgh*$^{-/-}$ mice would be decreased delivery of fatty acids from adipose tissue to the liver. Absence of TGH protein in WAT of *Tgh*$^{-/-}$ mice (Figure 4A) resulted in an approximately 70% decrease of total in vitro hydrolase activity in WAT homogenates (Figure 4B) and in a 70% increase of WAT weight (Figure 4C). Augmentation in WAT weight in *Tgh*$^{-/-}$ mice was accompanied with increased WAT cell size (Figure 4D). Despite the increased WAT, mass plasma fatty acid and glycerol concentrations in *Tgh*$^{-/-}$ mice were 30% lower in both fed and fasted conditions (Figures 4E–4H), indicating that lack of *Tgh* expression in WAT decreased TG mobilization in this tissue.

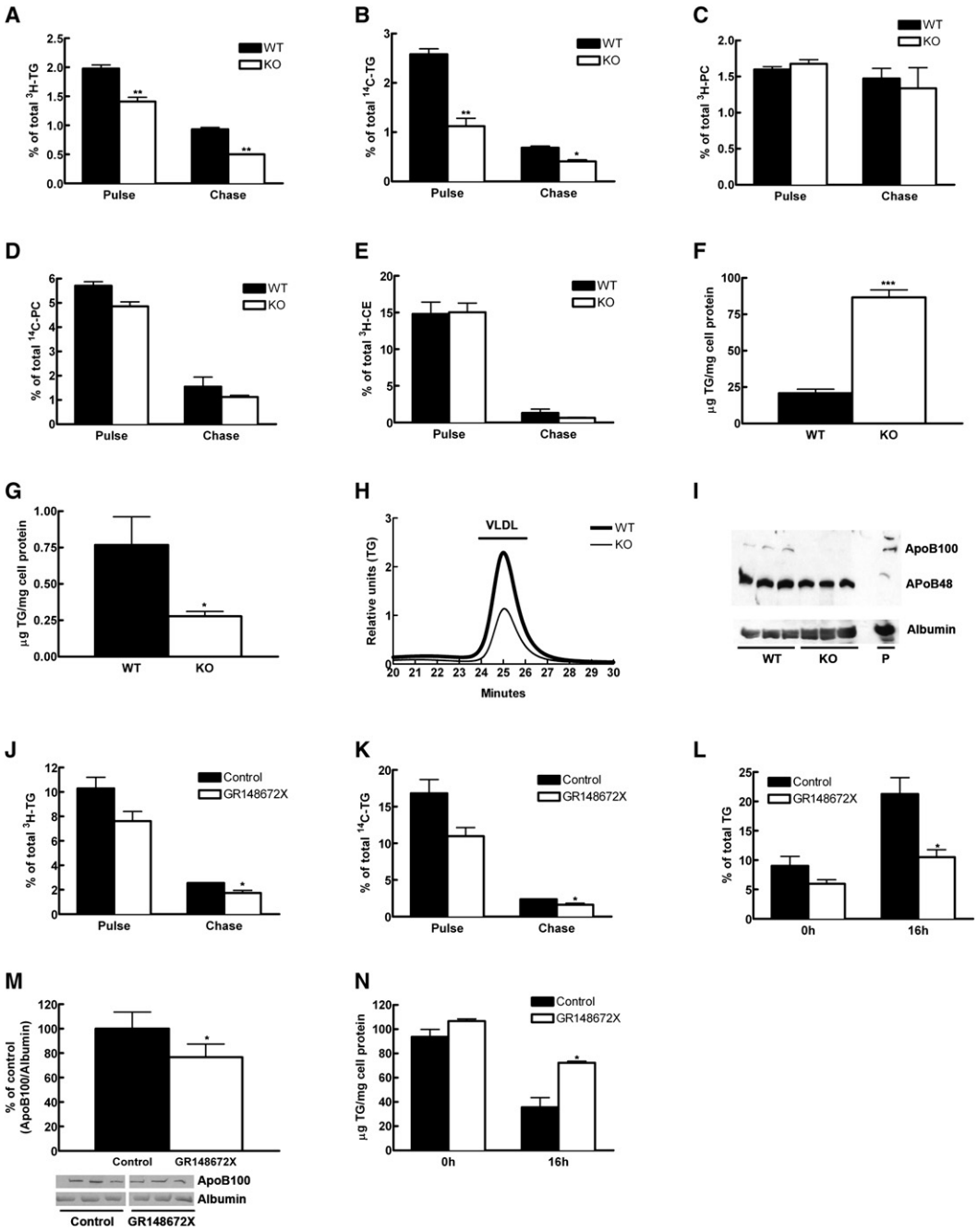

Figure 3. Decreased TG and ApoB Secretion from Hepatocytes Isolated from TGH-Deficient Mice and from Human Hepatocytes Treated with TGH-Specific Inhibitor

Secretion of TG, but not PC and CE, was reduced from primary hepatocytes from WT and *Tgh*$^{-/-}$ mice (A–E) and human hepatocytes treated with a TGH-specific inhibitor (J and K). TG accumulation in TGH-deficient mouse hepatocytes incubated with 0.4 mM OA (F) and in human hepatocytes (decreased TG turnover) treated with TGH-specific inhibitor (N). Decreased TG mass (G), VLDL-TG (H), and apoB100 (I) secretion from TGH-deficient hepatocytes and from TGH-inhibitor-treated primary human hepatocytes (L and M). Bars in (A)–(G) and (J)–(N) represent means ± SD. *p < 0.05, **p < 0.01, ***p < 0.001 versus WT.

Consistent with the increased WAT mass, plasma adiponectin levels were lower in both fasted and fed state in *Tgh*$^{-/-}$ mice (Table 1), while plasma levels of leptin and resistin were similar between the WT and *Tgh*$^{-/-}$ mice (Table 1). No differences were observed in plasma levels of inflammatory markers TNF-α and IL-6 (data not shown).

Increased Metabolic Rate in *Tgh*$^{-/-}$ Mice

Tgh$^{-/-}$ mice fed chow did not exhibit increased body weight (Figure 5A) despite significant increase in food intake compared to WT mice (Figure 5B). This is likely due to increased energy expenditure in *Tgh*$^{-/-}$ mice, as measured by oxygen consumption (Figure 5C). The augmented respiratory quotient (RQ)

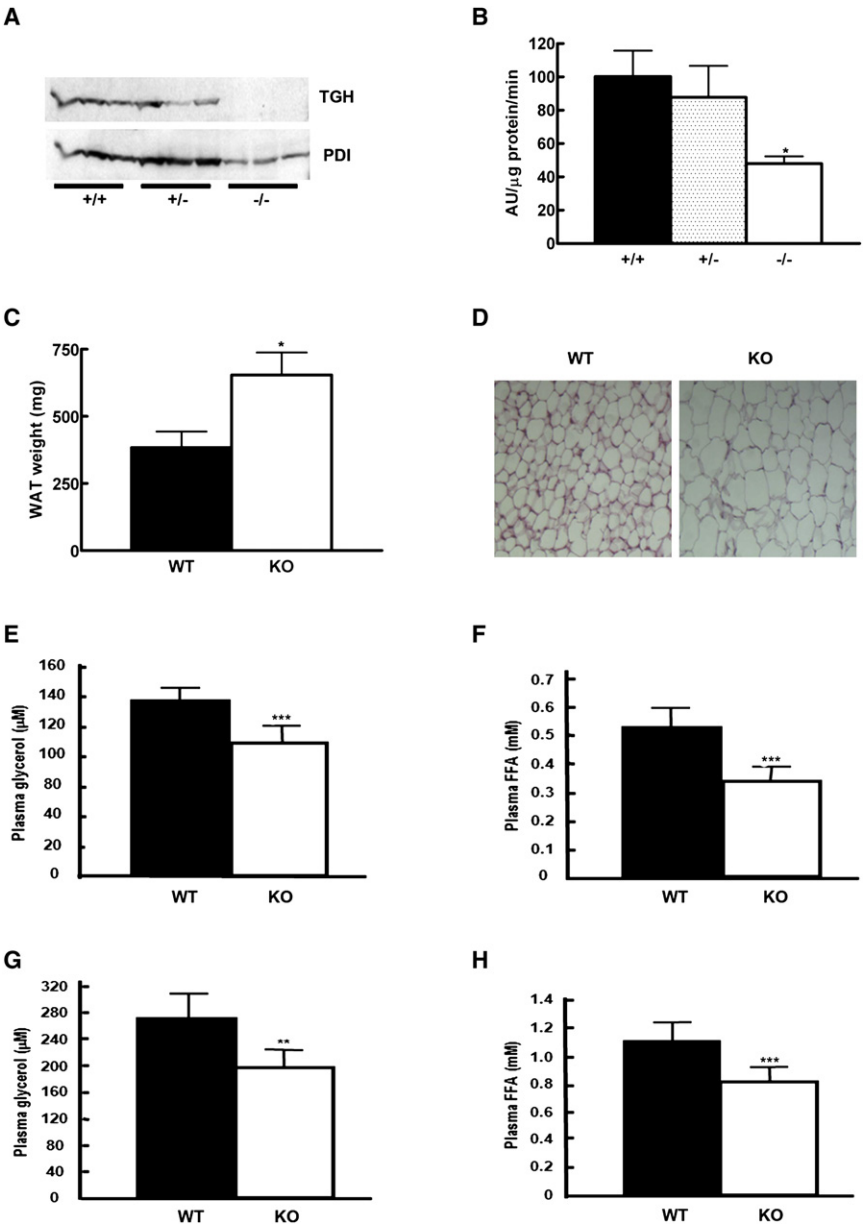

Figure 4. TGH-Deficient Mice Have Reduced Hydrolase Activity in WAT and Decreased Plasma Free Fatty Acid and Glycerol Levels

(A) Immunoblot of TGH and loading control (PDI) in WAT.

(B) Hydrolase activity in WAT homogenates.

(C) Epididymal WAT mass.

(D–H) (D) Histological analysis of WAT. Plasma glycerol levels in fed (E) and fasted (G) mice. Plasma FFA levels in fed (F) and fasted (H) mice. Ten-week-old female mice (n = 6) were analyzed. Bars in (B), (C), and (E)–(H) represent means ± SD. *p < 0.05, **p < 0.01, ***p < 0.001 versus WT.

(Figure 5D) indicates increased whole-body utilization of glucose and protein for energy production over lipid oxidation. These data are consistent with decreased fatty acid release from WAT in TGH-deficient mice. TGH-deficient mice also exhibited increased locomotor activity (Figure 5E), which may contribute to the increased energy consumption.

Improved Glucose Tolerance and Insulin Sensitivity

No significant changes in glucose or insulin levels were observed in TGH null mice when compared with control animals (Table 1). In oral glucose tolerance tests (Figure 6A), *Tgh*$^{-/-}$ mice displayed a markedly improved glucose tolerance compared with WT mice. In insulin tolerance tests (Figure 6B), the maximal decline of blood glucose levels was more pronounced in *Tgh*$^{-/-}$ mice (5.48 mmol/L) than in WT mice (3.44 mmol/L) and persisted during the entire measurement period. Improved insulin sensitivity in *Tgh*$^{-/-}$ mice resulted in decreased hepatic expression of gluconeogenic genes glucose-6-phosphatase (G6P) and phosphoenolpyruvate carboxykinase (PEPCK) during the fed state (Figure S4A) and in increased levels of the glycolytic enzyme glyceraldehyde-3-phosphate dehydrogenase (GAPDH) (Figure S4B).

Improved Pancreatic Islet Function in *Tgh*$^{-/-}$ Mice

Insulin secretion is sensitive to plasma and β cell lipid levels (Corkey et al., 1989; Mulder et al., 2004; Muoio and Newgard, 2006; Prentki et al., 1992; Yaney and Corkey, 2003). Mouse pancreatic β cells express low levels of TGH (Figures S4C and S4D), and ablation of *Tgh* expression did not affect islet intracellular lipase activity (Figure S4E) or TG levels (Figure S4F), possibly due to compensatory increased expression of *Hsl* (Figure S4G) and *Atgl* (Figure S4H), since the expression of TG synthetic genes *Dgat1* and *Dgat2* was not changed (Figures S4I and S4J). Islets isolated from *Tgh*$^{-/-}$ mice displayed normal glucose stimulated insulin secretion (Figure S4K). Immunohistochemistry of representative pancreatic sections showed a remarkable decrease in total islet area in *Tgh*$^{-/-}$ mice compared to WT mice (Figure 6C).

DISCUSSION

TG is required for proper assembly of secretion-competent apoB-containing lipoproteins (Adiels et al., 2008; Fisher and Ginsberg, 2002; Gibbons et al., 2000). In the absence of sufficient amounts of TG for VLDL assembly, apoB is targeted to degradation (Fisher and Ginsberg, 2002; Fisher et al., 1997). The goal of this study was to test the hypothesis that an ER-localized TGH plays an important role in VLDL assembly and energy metabolism in vivo. We found that ablation of *Tgh* expression resulted in the reduction of total liver carboxylester hydrolase

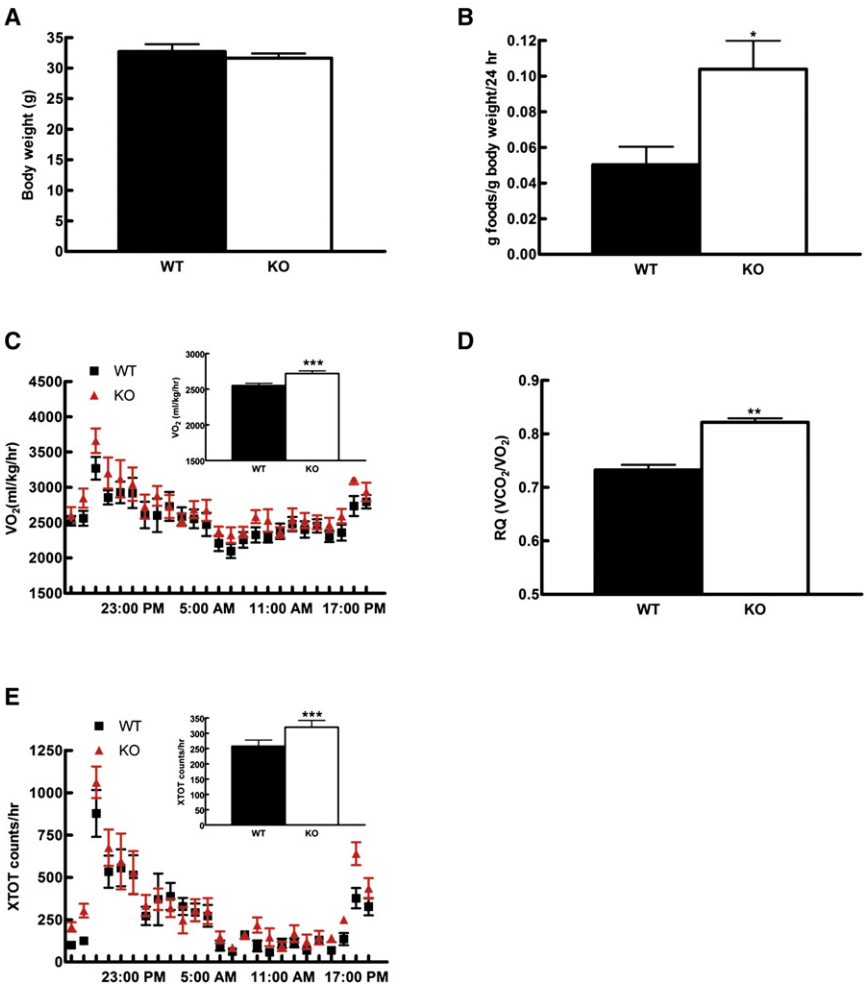

Figure 5. TGH-Deficient Mice Have Increased Energy Expenditure

Adult (20-week-old) male mice were used to analyze body weight (A); food intake (B); energy consumption, with inset showing mean ± SD over a 24 hr period (C); RQ (D); and locomotor activity, with inset showing mean ± SD over a 24 hr period (E). n = 6 for each group. Bars in (A)–(E) represent means ± SD. *$p < 0.05$, **$p < 0.01$, ***$p < 0.001$ versus WT.

activity by 30% and decreased plasma TG, FC, and CE levels in both fasted and fed state. Parallel decreases were found in plasma apoB100 levels. Lipidation of the secreted apoB100 was markedly diminished. Secretion of apoB48 was not affected, probably because unlike apoB100, apoB48 can enter the secretory pathway in a relatively poorly lipidated form. Surprisingly, we did not observe any differences in TG secretion rate between WT and *Tgh*−/− mice, although the ablation of *Tgh* expression decreased in vivo apoB100 secretion and reduced TG and apoB100 secretion from primary hepatocytes. Similar outcomes were observed using either Poloxamer-407 or Triton WR1339 methodologies. One possibility is that these methods might not have been sensitive enough to pick up changes in TG secretion that accompanied decreased secretion of apoB100. Unaltered rate of apoB48 secretion in vivo from $Tgh^{-/-}$ mice suggests that TG secretion associated with apoB48 could obscure the reduction of TG secretion associated with apoB100 in $Tgh^{-/-}$ mice. Our results support a role of TGH for the assembly of apoB100-lipoproteins. Unlike attenuation of VLDL secretion by the inhibition of MTP, which leads to fatty liver (Chandler et al., 2003; Cuchel et al., 2007; Raabe et al., 1999), ablation of *Tgh* expression does not provoke excessive hepatic TG deposition even during fasting. Although accretion of hepatic TG was not observed in vivo, the ablation of *Tgh* expression facilitated about 3-fold accumulation of TG in isolated hepatocytes incubated with exogenous fatty acid, indicating that TGH-mediated energy metabolism in other tissues is an important regulator of hepatic lipid levels.

Indeed, our previous studies have shown that attenuation of TGH activity in 3T3-L1 cells decreased fatty acid release without affecting glucose uptake (Wei et al., 2007b). In the fed state (when plasma insulin levels are high), adipose tissue HSL and ATGL are not active, but basal lipolysis continues (Haemmerle et al., 2006; Schweiger et al., 2006), possibly through the activity of TGH (Soni et al., 2004; Wei et al., 2007b). Therefore, absence of accumulation of hepatic TG levels in TGH-deficient mice might be a consequence of decreased TGH-mediated TG mobilization in WAT. Ablation of *Tgh* expression in WAT resulted in decreased hydrolase activity accompanied with reduced plasma fatty acid and glycerol levels. A reciprocal relationship exists between the use of fatty acids and glucose as substrates for energy production (Galgani et al., 2008). In agreement with decreased fatty acid release from WAT, TGH null mice exhibited increased RQ, which indicates overall preferential metabolism of carbohydrates over fatty acids. TGH null mice consumed significantly more energy compared to WT mice without body weight gain, which suggested altered energy metabolism. Indeed, $Tgh^{-/-}$ mice exhibited improved glucose tolerance and insulin sensitivity and increased locomotor activity. It is well known that high levels of circulating fatty acids result in abnormally high deposition of lipids in various organs (Bergman and Ader, 2000; Galgani et al., 2008). Excessive lipid infiltration of organs is believed to be one of the main causes of impaired insulin sensitivity in the liver, skeletal muscle, and pancreas (Bergman and Ader, 2000; Leclercq et al., 2007). It is probable that the observed reduction of fatty acid release from WAT in $Tgh^{-/-}$ mice is one of the reasons for the observed lack of TG accumulation in the liver and pancreatic β cells, leading to augmented insulin sensitivity. As a result, the expression of key enzymes related to hepatic gluconeogenesis, G6P and PEPCK, was reduced, suggesting that TGH deficiency leads to decreased hepatic glucose output and improved hepatic insulin sensitivity. It has been shown that

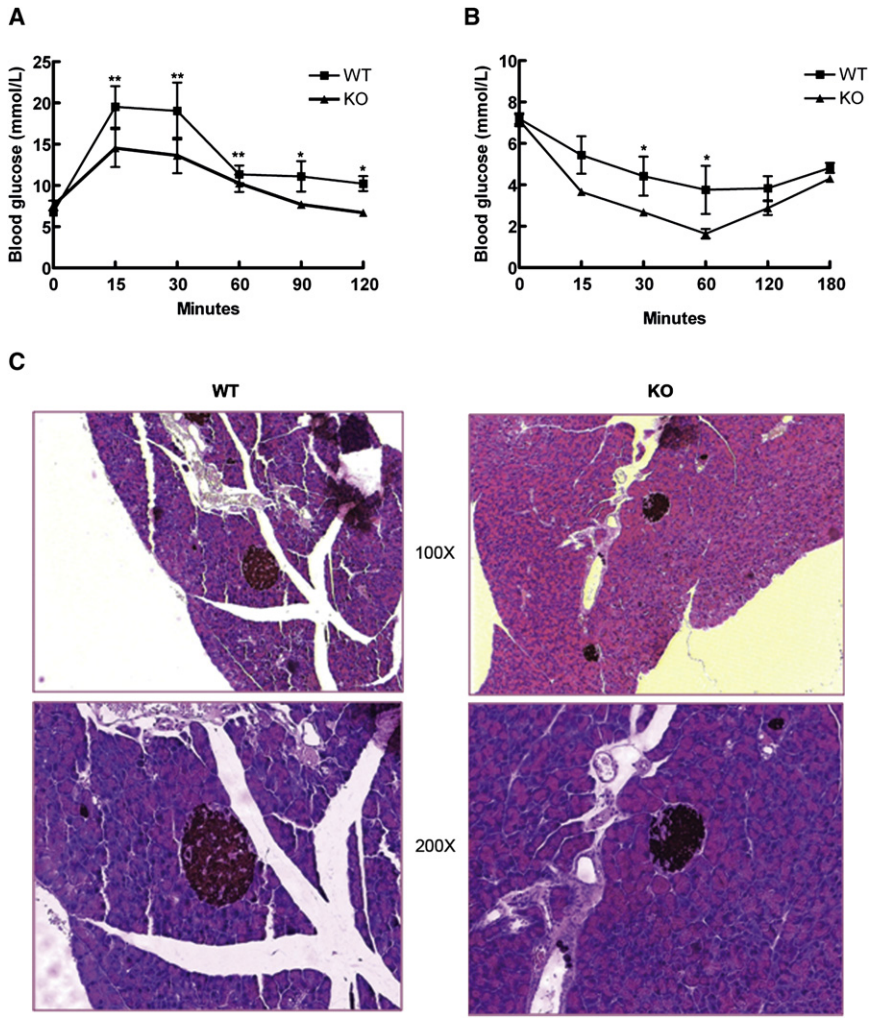

Figure 6. TGH-Deficient Mice Are More Glucose and Insulin Tolerant

(A and B) (A) Oral glucose and (B) insulin tolerance tests were performed in 10-week-old male mice (n = 6) fasted for 4 hr. Bars in (A) and (B) represent means ± SD. *p < 0.05, ***p < 0.001.

(C) Immunohistochemistry of pancreata.

exposure of β cells to high levels of fatty acids in vitro reduces glucose-stimulated insulin secretion, at least in part by inhibition of glucose oxidation and proinsulin transcription and translation (Cnop, 2008). In this study, we observed an ameliorated β cell function by TGH deficiency. The size of pancreatic islets is determined by the metabolic state. Under conditions of increased metabolic load, increased basal serum insulin levels, or obesity-associated insulin resistance, the islet size tends to become larger (Harada et al., 2003; Rhodes, 2005; Roduit et al., 2001; Shen et al., 2007). In agreement with the observed improved insulin and glucose tolerance in TGH-deficient mice, the islets in these mice were significantly smaller compared to WT mice.

Improved insulin sensitivity in TGH-deficient mice may be a consequence of ablation of *Tgh* expression in all tissues (liver, adipose tissue, and islets). The importance of TGH expression in individual tissues to the overall energy homeostasis will be answered by tissue-specific TGH knockout mice that are currently under development in our laboratory.

In conclusion, our results support a role of TGH not only in VLDL assembly but in the whole-body energy metabolism. Importantly, by using cultured primary human hepatocytes we show for the first time that our findings in mouse models recapitulate the behavior of the human TGH enzyme. Because TGH deficiency showed only positive effects on the overall energy homeostasis (decreased secretion of atherogenic lipoproteins without fatty liver, increased glucose tolerance, lower apparent metabolic insult to pancreatic β cells), TGH represents an ideal pharmacological target.

EXPERIMENTAL PROCEDURES

Generation of *Tgh*$^{-/-}$ Mice

A gene-targeting vector was designed to replace exon 5 that encodes the catalytic Ser_{221} residue (Dolinsky et al., 2001) with a neo cassette (Figure S1). An ~10.5 kb region used to construct the targeting vector was first cloned from a positively identified BAC clone. The region was designed such that the short homology arm (SA) extended 1.8 kb 3′ to exon 5. The long homology arm (LA) ended at the 5′ side of exon 5 and is 7.8 kb long. The Neo cassette replaced 850 bp of the gene, including exon 5. The targeting vector was confirmed by restriction analysis after each modification step and sequencing. Ten micrograms of the targeting vector were linearized by AscI and then transfected by electroporation of iTL 129SVev embryonic stem cells. After selection in G418, surviving clones were expanded for PCR analysis to identify recombinant ES clones. Primer A2 (5′-ACCAGCTGCCAGAGATTTCAG-3′) was designed downstream (3′) to the SA outside the region used to generate the targeting construct. PCR reactions using A2 with the N1 primer (5′-TGCG AGGCCAGAGGCCACTTGTGTAGC-3′) at the 5′ end of the Neo cassette amplifies a 2.3 kb fragment. *Tgh*$^{-/-}$ mice were also genotyped by a three-primer PCR reaction designed to distinguish homozygosity from heterozygosity, where the targeted allele gave a 2.4 kb fragment (primers N1 and A3 [5′-AGTTCATCCTCTGTCTTCTGG-3′]) and the wild-type allele gave a 2.9 kb fragment (primers 144F [5′-TCAGCCTTGACTCTTCTAACC-3′] and A3).

All animal procedures were approved by the University of Alberta's Animal Case and Use Committee and were in accordance with guidelines of the Canadian Council on Animal Care. Mice, housed three to five per cage, were exposed to a 12 hr light/dark cycle beginning with light at 8:00 a.m. Adult male and female mice were fed ad libitum a chow diet from LabDiet (PICO laboratory Rodent Diet 20) and had a free access to water. Adult male (12- to 24-week-old) mice, all background (129P2) and age matched, were used in the experiments unless specified otherwise.

Blood and Plasma Parameters

Blood samples were collected from tail veins. Plasma levels of TG, FC, CEs, and phospholipids were determined by gas chromatography. Blood glucose was monitored using blood glucose strips and the Accu-Check glucometer (Roche Diagnostics, Vienna, Austria). Plasma concentrations of insulin, leptin, resistin, TNF-α, and IL-6 were measured using Mouse Serum Adipokine Lincoplex kit. Plasma adiponectin concentrations were determined using mouse

adiponectin radioimmunoassay. All adipokine and cytokine measurements were performed by Millipore Corporation, Billerica, MA. Plasma fatty acid levels were determined using NEFA C commercial kit according to the manufacturer's protocol (Wako Chemicals GmbH, USA). Plasma glycerol levels were determined using the Serum Triglyceride Determination Kit (Sigma, USA).

RNA Isolation and PCR Analysis

Total RNA was isolated using Trizol reagent (Life Technologies, Inc.). First-strand cDNA synthesis from 2 μg of total RNA was performed using Super-Script II reverse transcriptase (Invitrogen) primed by oligo(dT)$_{12–18}$ primers. The transcripts of TGH, Es-x, and Es-22 were evaluated by PCR analysis. Real-time qPCR was employed to detect other transcripts related to fatty acid oxidation, lipogenesis, gluconeogenesis, glycolysis, and lipolysis. Detailed procedures for real-time qPCR are presented in the Supplemental Information. All primers were synthesized at the DNA Core Facility of the University of Alberta. Primers for the various genes are listed in Table S1.

Carboxylester Hydrolase Activity Assay

Tissues were homogenized in 50 mM Tris-HCl (pH 7.4), 250 mM sucrose, and 1 mM EDTA, using a glass/Teflon homogenizer followed by sonication for 20 s. A fluorescence-based assay using 4-methyl umbelliferyl heptanoate (MUH) as a substrate was performed essentially as described previously (Alam et al., 2006; Gilham et al., 2005; Gilham and Lehner, 2005).

Determination of Tissue Lipids

The mass of tissue TG, phospholipids, cholesterol, and CEs was determined by gas chromatography as described previously (Sahoo et al., 2004; Wei et al., 2007a).

Hepatic TG and ApoB Production In Vivo

Mice were fasted for 4 hr and injected with 100 μl of PBS containing 250 μCi of [^{35}S]methionine via tail vein, and P-407 (1000 mg/kg body weight) in saline was injected intraperitoneally. One hundred microliters of blood was taken before and 1 hr after injection. Two hours following the injection of P-407, time that was shown to be in the linear range for hepatic TG and apoB production (Millar et al., 2005), blood samples were collected and plasma was isolated and processed for analyses as described as follows. To 100 μl of plasma were added 800 μl of PBS, 100 μl 10× immunoprecipitation buffer (1.5 M NaCl, 0.5 M Tris·Cl [pH 7.4], 50 mM EDTA, 5% [v/v] Triton X-100 and 1% [w/v] SDS) and 10 μl goat anti-human apoB IgG. The mixture was incubated on a rotating rack overnight at 4°C, after which 50 μl of protein A Sepharose was added and the mixture was further incubated for 3 hr. The beads were pelleted by brief centrifugation and were washed three times with excess immunoprecipitation buffer, followed by denaturing electrophoresis sample buffer. Samples were boiled and underwent electrophoresis in SDS 5% polyacrylamide gels. Gels were stained by Coomassie blue, dried, and exposed to X-ray films. Equal aliquots of plasma samples were also immunoprecipitated with goat anti-human apoB antibodies and separated by electrophoresis; apoB48 and apoB100 proteins were visualized by Coomassie blue, excised, and dissolved at 60°C in 0.2 ml of 60% perchloric acid followed by 0.4 ml of 30% hydrogen peroxide (Gilham et al., 2003; Lehner and Vance, 1999). Radioactivity associated with apoB48 and apoB100 was determined by using the Hionic-Fluor scintillation cocktail (Packard Instrument, Meriden, CT) and scintillation counting. The total radioactivity in plasma before immunoprecipitation was also determined.

Plasma at 2 hr after injection of P-407 was subjected to ultracentrifugation to isolate apoB-containing lipoprotein of various densities (Kulinski et al., 2002). Brieftly, 200 μl of pooled plasma samples collected from WT and *Tgh*$^{-/-}$ mice were combined with 1.3 ml of PBS, mixed with 0.7 g of KBr, and placed in a 5.0 ml Quick-Seal tube. The sample was overlaid with 3.5 ml of 0.9% NaCl. The samples were centrifuged at 416,000 × g for 1 hr in a VTi 65.2 rotor. Ten fractions, 0.5 ml each, with densities ranging from 1.006 g/ml (fraction 10) to 1.21 g/ml (fraction 1), were collected from the bottom of the tube. ApoB was precipitated by Cab-O-Sil from each fraction and analyzed by electrophoresis on SDS 5% polyacrylamide gels. The gel was stained, dried, and exposed to X-ray film.

Isolation of Primary Hepatocytes

Primary mouse hepatocytes were isolated by collagenase perfusion of the livers from male wild-type (WT) and *Tgh*$^{-/-}$ mice that had been fed ad libitum. Hepatocytes were plated on collagen-coated 60 mm dishes (Corning, Nepean, Ontario, Canada) at 2.0 × 10^6 cells/dish and incubated for 5 hr in DMEM containing 15% FBS at 37°C in humidified air containing 5% CO_2 to allow cells to attach.

Human hepatocytes were prepared by dissociation of liver fragments obtained from hepatectomies performed for therapeutic purposes at the Service of Digestive Tract Surgery, University of Alberta. The operations were performed for intrahepatic hemangioma, colorectal metastasis, or benign liver tumor; segments of human liver tissue (15–20 cm^3) were obtained from resection specimens far away from the tumor margin. All patients gave their consent to participate. The study was approved by the University of Alberta Ethics Committee. Cell counts (hemocytometer) and viability (trypan blue exclusion) were confirmed before use; viability was routinely >80%.

Hepatic Lipid Turnover and Secretion

Primary mouse hepatocytes were incubated for 4 hr in 2 ml of DMEM containing 5 μCi [^{3}H]OA complexed with 0.4 mM OA/ 0.5% fatty acid-free BSA and 0.5 μCi [^{14}C]glycerol. After the 4 hr incubation, some cells and media were collected for analysis (pulse). Remaining dishes were washed with PBS and incubated for 1 hr with DMEM to allow secretion of lipoproteins containing newly synthesized lipids. Cells were then incubated with DMEM for 4 hr and cells and media were collected for analysis of secretion of preformed lipids (chase). Lipids were extracted, resolved by thin-layer chromatography, and analyzed as described in the Supplemental Information. To evaluate the lipid mass secreted by primary hepatocytes, cells were incubated with 2 ml DMEM containing 0.4 mM OA/ 0.5% fatty acid-free BSA for 16 hr. After incubation, cells and media were collected for lipid analysis by gas chromatography and lipoprotein profile analysis by FPLC (Sahoo et al., 2004; Wei et al., 2007a).

Incubations of primary human hepatocytes were performed as described above for mouse hepatocytes except that 10 μM TGH-specific inhibitor GR148672X was included as specified.

Secretion of ApoB from Primary Hepatocytes

Primary mouse hepatocytes were incubated for 4 hr with DMEM containing 0.4 mM OA complexed to 0.5% BSA in order to increase intracellular TG stores. Cells were then washed and incubated for 16 hr with 2 ml of DMEM. Media were removed and briefly centrifuged to remove cellular debris. Lipid mass in cells and media was determined using gas chromatography. Apolipoproteins and albumin were collected from media by Cab-O-Sil and analyzed by immunoblotting (Gilham et al., 2003).

Metabolic Measurements

Measurements of oxygen consumption (VO_2) and RQ with indirect calorimetry were performed on mice at 20 weeks of age. Animals were maintained on a standard chow diet under 12 hr light and dark cycles beginning at 6:00 a.m. and 6:00 p.m., respectively. Mice were acclimated in individual chambers for 2 days before recording. Measurements of VO_2 were recorded every 14 min over 2 days using the Oxymax System (Columbus Instruments, Columbus, OH). RQ equals volumes of CO_2 released/volumes of O_2 consumed.

Oral Glucose Tolerance and Insulin Tolerance

Prior to oral glucose tolerance, mice were fasted for 3 hr. Then a dextrose solution (3 mg/g body weight) was administered by oral gavage. Glucose levels were monitored before and at 15, 30, 60, and 120 min postgavage using blood glucose strips (Roche Diagnostics, Vienna, Austria).

For insulin sensitivity determinations, mice were fasted for 4 hr and injected intraperitoneally with 1 U bovine insulin/kg of body weight. Blood was collected before injection and 15, 30, 60, 120 min after injection, and glucose levels were determined as described above.

Immunohistochemical Analysis of Pancreata

Pancreas was removed using standard blunt dissection techniques and placed in Z-fix for 24 hr, embedded in paraffin, and sectioned at 3 μm thickness onto Histobond slides. The resulting slides were stained for insulin-positive cells

using standard ABC-DAB immunohistochemistry techniques and observed under a standard light microscope as previously described (Korbutt et al., 1996).

Statistical Analysis

Data are presented as means ± SD employing unpaired two-tailed t test. Oral glucose tolerance test, insulin sensitivity test, VO2, and RQ were analyzed by two-way ANOVA followed by Bonferroni post test (GraphPad PRISM 4 software). Five to six animals were used in each experimental group. $P < 0.05$ was interpreted as a significant difference.

SUPPLEMENTAL INFORMATION

Supplemental Information includes Supplemental Experimental Procedures, Supplemental References, four figures, and one table and can be found with this article online at doi:10.1016/j.cmet.2010.02.005.

ACKNOWLEDGMENTS

We thank Johanne Lamoureux, Lena Li, Priscilla Gao, Audric Moses, and Laura Hargreaves for technical assistance and Dr. Simonetta Sipione for critical reading of the manuscript. Human hepatocytes were kindly provided by Dr. Norm Kneteman (University of Alberta). E.W. was supported by the Canadian Institutes of Health Research (CIHR) Strategic Training Program (SCOLAR); H.W. was supported by studentships from the Heart and Stroke Foundation of Canada and from the Alberta Heritage Foundation for Medical Research. Y.B.A. and V.W.D. were supported by postdoctoral fellowships from the Alberta Heritage Foundation for Medical Research. This work was supported by a CIHR grant (MOP-69043). R.L., J.R.B.D., and G.S.K. are Senior Scholars of the Alberta Heritage Foundation for Medical Research. J.R.B.D. holds a Canada Research Chair in Molecular Biology of Heart Disease and Metabolism.

Received: August 6, 2008
Revised: December 3, 2009
Accepted: February 8, 2010
Published: March 2, 2010

REFERENCES

Adiels, M., Olofsson, S.O., Taskinen, M.R., and Boren, J. (2008). Overproduction of very low-density lipoproteins is the hallmark of the dyslipidemia in the metabolic syndrome. Arterioscler. Thromb. Vasc. Biol. *28*, 1225–1236.

Alam, M., Gilham, D., Vance, D.E., and Lehner, R. (2006). Mutation of F417 but not of L418 or L420 in the lipid binding domain decreases the activity of triacylglycerol hydrolase. J. Lipid Res. *47*, 375–383.

Bergman, R.N., and Ader, M. (2000). Free fatty acids and pathogenesis of type 2 diabetes mellitus. Trends Endocrinol. Metab. *11*, 351–356.

Carmena, R., Duriez, P., and Fruchart, J.C. (2004). Atherogenic lipoprotein particles in atherosclerosis. Circulation *109*, III2–III7.

Chahil, T.J., and Ginsberg, H.N. (2006). Diabetic dyslipidemia. Endocrinol. Metab. Clin. North Am. *35*, 491–510.

Chandler, C.E., Wilder, D.E., Pettini, J.L., Savoy, Y.E., Petras, S.F., Chang, G., Vincent, J., and Harwood, H.J., Jr. (2003). CP-346086: an MTP inhibitor that lowers plasma cholesterol and triglycerides in experimental animals and in humans. J. Lipid Res. *44*, 1887–1901.

Chen, H.C., and Farese, R.V., Jr. (2005). Inhibition of triglyceride synthesis as a treatment strategy for obesity: lessons from DGAT1-deficient mice. Arterioscler. Thromb. Vasc. Biol. *25*, 482–486.

Cnop, M. (2008). Fatty acids and glucolipotoxicity in the pathogenesis of type 2 diabetes. Biochem. Soc. Trans. *36*, 348–352.

Corkey, B.E., Glennon, M.C., Chen, K.S., Deeney, J.T., Matschinsky, F.M., and Prentki, M. (1989). A role for malonyl-CoA in glucose-stimulated insulin secretion from clonal pancreatic beta-cells. J. Biol. Chem. *264*, 21608–21612.

Cuchel, M., Bloedon, L.T., Szapary, P.O., Kolansky, D.M., Wolfe, M.L., Sarkis, A., Millar, J.S., Ikewaki, K., Siegelman, E.S., Gregg, R.E., and Rader, D.J. (2007). Inhibition of microsomal triglyceride transfer protein in familial hypercholesterolemia. N. Engl. J. Med. *356*, 148–156.

Dolinsky, V.W., Sipione, S., Lehner, R., and Vance, D.E. (2001). The cloning and expression of a murine triacylglycerol hydrolase cDNA and the structure of its corresponding gene. Biochim. Biophys. Acta *1532*, 162–172.

Dolinsky, V.W., Douglas, D.N., Lehner, R., and Vance, D.E. (2004a). Regulation of the enzymes of hepatic microsomal triacylglycerol lipolysis and re-esterification by the glucocorticoid dexamethasone. Biochem. J. *378*, 967–974.

Dolinsky, V.W., Gilham, D., Alam, M., Vance, D.E., and Lehner, R. (2004b). Triacylglycerol hydrolase: role in intracellular lipid metabolism. Cell. Mol. Life Sci. *61*, 1633–1651.

Fisher, E.A., Zhou, M., Mitchell, D.M., Wu, X., Omura, S., Wang, H., Goldberg, A.L., and Ginsberg, H.N. (1997). The degradation of apolipoprotein B100 is mediated by the ubiquitin-proteasome pathway and involves heat shock protein 70. J. Biol. Chem. *272*, 20427–20434.

Fisher, E.A., and Ginsberg, H.N. (2002). Complexity in the secretory pathway: the assembly and secretion of apolipoprotein B-containing lipoproteins. J. Biol. Chem. *277*, 17377–17380.

Galgani, J.E., Moro, C., and Ravussin, E. (2008). Metabolic flexibility and insulin resistance. Am. J. Physiol. Endocrinol. Metab. *295*, E1009–E1017.

Gibbons, G.F., Islam, K., and Pease, R.J. (2000). Mobilisation of triacylglycerol stores. Biochim. Biophys. Acta *1483*, 37–57.

Gibbons, G.F., Wiggins, D., Brown, A.M., and Hebbachi, A.M. (2004). Synthesis and function of hepatic very-low-density lipoprotein. Biochem. Soc. Trans. *32*, 59–64.

Gilham, D., and Lehner, R. (2005). Techniques to measure lipase and esterase activity in vitro. Methods *36*, 139–147.

Gilham, D., Ho, S., Rasouli, M., Martres, P., Vance, D.E., and Lehner, R. (2003). Inhibitors of hepatic microsomal triacylglycerol hydrolase decrease very low density lipoprotein secretion. FASEB J. *17*, 1685–1687.

Gilham, D., Alam, M., Gao, W., Vance, D.E., and Lehner, R. (2005). Triacylglycerol hydrolase is localized to the endoplasmic reticulum by an unusual retrieval sequence where it participates in VLDL assembly without utilizing VLDL lipids as substrates. Mol. Biol. Cell *16*, 984–996.

Ginsberg, H.N., Zhang, Y.L., and Hernandez-Ono, A. (2005). Regulation of plasma triglycerides in insulin resistance and diabetes. Arch. Med. Res. *36*, 232–240.

Haemmerle, G., Lass, A., Zimmermann, R., Gorkiewicz, G., Meyer, C., Rozman, J., Heldmaier, G., Maier, R., Theussl, C., Eder, S., et al. (2006). Defective lipolysis and altered energy metabolism in mice lacking adipose triglyceride lipase. Science *312*, 734–737.

Harada, K., Shen, W.J., Patel, S., Natu, V., Wang, J., Osuga, J., Ishibashi, S., and Kraemer, F.B. (2003). Resistance to high-fat diet-induced obesity and altered expression of adipose-specific genes in HSL-deficient mice. Am. J. Physiol. Endocrinol. Metab. *285*, E1182–E1195.

Havel, R.J. (1990). Role of triglyceride-rich lipoproteins in progression of atherosclerosis. Circulation *81*, 694–696.

Hussain, M.M., Shi, J., and Dreizen, P. (2003). Microsomal triglyceride transfer protein and its role in apoB-lipoprotein assembly. J. Lipid Res. *44*, 22–32.

Korbutt, G.S., Elliott, J.F., Ao, Z., Smith, D.K., Warnock, G.L., and Rajotte, R.V. (1996). Large scale isolation, growth, and function of porcine neonatal islet cells. J. Clin. Invest. *97*, 2119–2129.

Kulinski, A., Rustaeus, S., and Vance, J.E. (2002). Microsomal triacylglycerol transfer protein is required for lumenal accretion of triacylglycerol not associated with ApoB, as well as for ApoB lipidation. J. Biol. Chem. *277*, 31516–31525.

Leclercq, I.A., Da Silva Morais, A., Schroyen, B., Van Hul, N., and Geerts, A. (2007). Insulin resistance in hepatocytes and sinusoidal liver cells: mechanisms and consequences. J. Hepatol. *47*, 142–156.

Lehner, R., and Vance, D.E. (1999). Cloning and expression of a cDNA encoding a hepatic microsomal lipase that mobilizes stored triacylglycerol. Biochem. J. *343*, 1–10.

Lehner, R., and Verger, R. (1997). Purification and characterization of a porcine liver microsomal triacylglycerol hydrolase. Biochemistry *36*, 1861–1868.

Lieu, H.D., Withycombe, S.K., Walker, Q., Rong, J.X., Walzem, R.L., Wong, J.S., Hamilton, R.L., Fisher, E.A., and Young, S.G. (2003). Eliminating atherogenesis in mice by switching off hepatic lipoprotein secretion. Circulation *107*, 1315–1321.

Marchesini, G., Marzocchi, R., Agostini, F., and Bugianesi, E. (2005). Nonalcoholic fatty liver disease and the metabolic syndrome. Curr. Opin. Lipidol. *16*, 421–427.

Millar, J.S., Cromley, D.A., McCoy, M.G., Rader, D.J., and Billheimer, J.T. (2005). Determining hepatic triglyceride production in mice: comparison of poloxamer 407 with Triton WR-1339. J. Lipid Res. *46*, 2023–2028.

Millar, J.S., Stone, S.J., Tietge, U.J., Tow, B., Billheimer, J.T., Wong, J.S., Hamilton, R.L., Farese, R.V., Jr., and Rader, D.J. (2006). Short-term overexpression of DGAT1 or DGAT2 increases hepatic triglyceride but not VLDL triglyceride or apoB production. J. Lipid Res. *47*, 2297–2305.

Monetti, M., Levin, M.C., Watt, M.J., Sajan, M.P., Marmor, S., Hubbard, B.K., Stevens, R.D., Bain, J.R., Newgard, C.B., Farese, R.V., Sr.., et al. (2007). Dissociation of hepatic steatosis and insulin resistance in mice overexpressing DGAT in the liver. Cell Metab. *6*, 69–78.

Mulder, H., Yang, S., Winzell, M.S., Holm, C., and Ahren, B. (2004). Inhibition of lipase activity and lipolysis in rat islets reduces insulin secretion. Diabetes *53*, 122–128.

Muoio, D.M., and Newgard, C.B. (2006). Obesity-related derangements in metabolic regulation. Annu. Rev. Biochem. *75*, 367–401.

Owen, M., and Zammit, V.A. (1997). Evidence for overt and latent forms of DGAT in rat liver microsomes. Implications for the pathways of triacylglycerol incorporation into VLDL. Biochem. Soc. Trans. *25*, 21S.

Petersen, K.F., and Shulman, G.I. (2006). Etiology of insulin resistance. Am. J. Med. *119*, S10–S16.

Prentki, M., Vischer, S., Glennon, M.C., Regazzi, R., Deeney, J.T., and Corkey, B.E. (1992). Malonyl-CoA and long chain acyl-CoA esters as metabolic coupling factors in nutrient-induced insulin secretion. J. Biol. Chem. *267*, 5802–5810.

Raabe, M., Veniant, M.M., Sullivan, M.A., Zlot, C.H., Bjorkegren, J., Nielsen, L.B., Wong, J.S., Hamilton, R.L., and Young, S.G. (1999). Analysis of the role of microsomal triglyceride transfer protein in the liver of tissue-specific knockout mice. J. Clin. Invest. *103*, 1287–1298.

Rhodes, C.J. (2005). Type 2 diabetes—a matter of beta-cell life and death? Science *307*, 380–384.

Roduit, R., Masiello, P., Wang, S.P., Li, H., Mitchell, G.A., and Prentki, M. (2001). A role for hormone-sensitive lipase in glucose-stimulated insulin secretion: a study in hormone-sensitive lipase-deficient mice. Diabetes *50*, 1970–1975.

Sahoo, D., Trischuk, T.C., Chan, T., Drover, V.A., Ho, S., Chimini, G., Agellon, L.B., Agnihotri, R., Francis, G.A., and Lehner, R. (2004). ABCA1-dependent lipid efflux to apolipoprotein A-I mediates HDL particle formation and decreases VLDL secretion from murine hepatocytes. J. Lipid Res. *45*, 1122–1131.

Savage, D.B., Petersen, K.F., and Shulman, G.I. (2007). Disordered lipid metabolism and the pathogenesis of insulin resistance. Physiol. Rev. *87*, 507–520.

Schaefer, E.J., McNamara, J.R., Shah, P.K., Nakajima, K., Cupples, L.A., Ordovas, J.M., and Wilson, P.W. (2002). Elevated remnant-like particle cholesterol and triglyceride levels in diabetic men and women in the Framingham Offspring Study. Diabetes Care *25*, 989–994.

Schweiger, M., Schreiber, R., Haemmerle, G., Lass, A., Fledelius, C., Jacobsen, P., Tornqvist, H., Zechner, R., and Zimmermann, R. (2006). Adipose triglyceride lipase and hormone-sensitive lipase are the major enzymes in adipose tissue triacylglycerol catabolism. J. Biol. Chem. *281*, 40236–40241.

Shen, W.J., Liang, Y., Wang, J., Harada, K., Patel, S., Michie, S.A., Osuga, J., Ishibashi, S., and Kraemer, F.B. (2007). Regulation of hormone-sensitive lipase in islets. Diabetes Res. Clin. Pract. *75*, 14–26.

Smith, S.J., Cases, S., Jensen, D.R., Chen, H.C., Sande, E., Tow, B., Sanan, D.A., Raber, J., Eckel, R.H., and Farese, R.V., Jr. (2000). Obesity resistance and multiple mechanisms of triglyceride synthesis in mice lacking Dgat. Nat. Genet. *25*, 87–90.

Soni, K.G., Lehner, R., Metalnikov, P., O'Donnell, P., Semache, M., Gao, W., Ashman, K., Pshezhetsky, A.V., and Mitchell, G.A. (2004). Carboxylesterase 3 (EC 3.1.1.1) is a major adipocyte lipase. J. Biol. Chem. *279*, 40683–40689.

Stone, S.J., Myers, H.M., Watkins, S.M., Brown, B.E., Feingold, K.R., Elias, P.M., and Farese, R.V., Jr. (2004). Lipopenia and skin barrier abnormalities in DGAT2-deficient mice. J. Biol. Chem. *279*, 11767–11776.

Tietge, U.J., Bakillah, A., Maugeais, C., Tsukamoto, K., Hussain, M., and Rader, D.J. (1999). Hepatic overexpression of microsomal triglyceride transfer protein (MTP) results in increased in vivo secretion of VLDL triglycerides and apolipoprotein B. J. Lipid Res. *40*, 2134–2139.

Vukmirica, J., Tran, K., Liang, X., Shan, J., Yuan, J., Miskie, B.A., Hegele, R.A., Resh, M.D., and Yao, Z. (2003). Assembly and secretion of very low density lipoproteins containing apolipoprotein B48 in transfected McA-RH7777 cells. Lack of evidence that palmitoylation of apolipoprotein B48 is required for lipoprotein secretion. J. Biol. Chem. *278*, 14153–14161.

Wang, S., McLeod, R.S., Gordon, D.A., and Yao, Z. (1996). The microsomal triglyceride transfer protein facilitates assembly and secretion of apolipoprotein B-containing lipoproteins and decreases cotranslational degradation of apolipoprotein B in transfected COS-7 cells. J. Biol. Chem. *271*, 14124–14133.

Wang, H., Gilham, D., and Lehner, R. (2007). Proteomic and lipid characterization of apolipoprotein B-free luminal lipid droplets from mouse liver microsomes: implications for very low density lipoprotein assembly. J. Biol. Chem. *282*, 33218–33226.

Wei, E., Alam, M., Sun, F., Agellon, L.B., Vance, D.E., and Lehner, R. (2007a). Apolipoprotein B and triacylglycerol secretion in human triacylglycerol hydrolase transgenic mice. J. Lipid Res. *48*, 2597–2606.

Wei, E., Gao, W., and Lehner, R. (2007b). Attenuation of adipocyte triacylglycerol hydrolase activity decreases basal fatty acid efflux. J. Biol. Chem. *282*, 8027–8035.

Wiggins, D., and Gibbons, G.F. (1992). The lipolysis/esterification cycle of hepatic triacylglycerol. Its role in the secretion of very-low-density lipoprotein and its response to hormones and sulphonylureas. Biochem. J. *284*, 457–462.

Yaney, G.C., and Corkey, B.E. (2003). Fatty acid metabolism and insulin secretion in pancreatic beta cells. Diabetologia *46*, 1297–1312.

Yang, L.Y., Kuksis, A., Myher, J.J., and Steiner, G. (1995). Origin of triacylglycerol moiety of plasma very low density lipoproteins in the rat: structural studies. J. Lipid Res. *36*, 125–136.

Yang, L.Y., Kuksis, A., Myher, J.J., and Steiner, G. (1996). Contribution of de novo fatty acid synthesis to very low density lipoprotein triacylglycerols: evidence from mass isotopomer distribution analysis of fatty acids synthesized from [2H6]ethanol. J. Lipid Res. *37*, 262–274.